Plasma Chemistry and Plasma Processing, Vol. 25, No. 6, December 2005 (© 2005)
DOI: 10.1007/s11090-005-6804-1

Influence of Ferroelectric Materials and Catalysts on the Performance of Non-Thermal Plasma (NTP) for the Removal of Air Pollutants

F. Holzer,[1] F.D. Kopinke,[1] and U. Roland[1,2]

Received January 19, 2005; revised May 10, 2005

The introduction of ferroelectric and catalytically active materials into the discharge zone of NTP reactors is a promising way to improve their performance for the removal of hazardous substances, especially those appearing in low concentrations. In this study, several coaxial barrier-discharge plasma reactors varying in size and barrier material (glass, Al_2O_3, and TiO_2) were used. The oxidation of methyl tert-butyl ether (MTBE), toluene and acetone was studied in a gas-phase plasma and in various packed-bed reactors (filled with ferroelectric and catalytically active materials). In the ferroelectric packed-bed reactors, better energy efficiency and CO_2 selectivity were found for the oxidation of the model substances. Studies on the oxidation of a toluene/acetone mixture in air showed an enhanced oxidation of the less reactive acetone related to toluene in the ferroelectric packed-bed reactors. It can be concluded that the change of the electrical discharge behaviour was caused by a larger number of non-selective and highly reactive plasma species formed within the ferroelectric bed. When combining ferroelectric ($BaTiO_3$) and catalytically active materials ($LaCoO_3$), only a layered implementation led to synergistic effects utilising both highly energetic species formed in the ferroelectric packed-bed and the potential for total oxidation provided by the catalytically active material in the second part of the packed bed.

KEY WORDS: Non-thermal plasma; atmospheric pressure; VOCs; ferroelectric pellets; plasma catalysis; CO_2 selectivity.

1. INTRODUCTION

The application of non-thermal plasma (NTP) offers a great potential either to remove hazardous compounds or to produce chemicals in the gas phase due to the direct energy transfer by highly accelerated electrons.

[1]Department of Environmental Technology, UFZ Centre for Environmental Research, Leipzig-Halle, Permoserstr. 15, D-04318 Leipzig, Germany.
[2]To whom correspondence should be addressed. Telephone: +49 (341) 235 2581; fax: +49 (341) 235 2492; e-mail: ulf.roland@ufz.de

By overcoming the activation barrier of the desired processes under non-equilibrium conditions (with "hot" electrons or other reactive species and "cold" neutral gas molecules), the specific energy input can be minimised.

The NTPs have already been applied to remove aliphatic,[1–3] aromatic[3,4] and halogenated hydrocarbons[5–8] as well as inorganic pollutants such as SO_2, H_2S and NO_x[9–12] from gas streams. On the other hand, NTPs have also been successfully applied for the production of chemicals (e.g. methanol from methane[13,14] and other selective-oxidation reactions),[15] reforming[7,16] and reduction of supported metal catalysts.[17]

Unfortunately, on the basis of a large number of experimental results it has to be recognised that a non-thermal gas-phase plasma does not usually allow achieving both high conversion and satisfactory selectivity, which hitherto prevented a broader application of this technology. For instance, typical values between 0.3 and 0.7 for the selectivity of the oxidation to CO_2, which is defined as

$$S_{CO_2} = \frac{[CO_2]}{[CO_x] + [C_{org}]} \tag{1}$$

have been described in the literature.[1,2,18,19] Due to the non-equilibrium conditions, even a reduction of CO_2 to CO ($[CO/CO_2] \approx 0.25$) occurs in an air atmosphere.[19,20] Therefore, it can be stated that carbon monoxide is one of the major immanent products of hydrocarbon oxidation in non-thermal gas-phase plasmas.

In many cases, the number of radicals produced in NTP seems to be limited. This cannot be overcome by only varying the NTP type alone. For the reduction of NO as a standard reaction, Penetrante *et al.*[21,22] have shown that the specific energy consumption is almost independent of the applied discharge (corona, barrier or packed-bed) and of the voltage type (50 Hz sinusoidal or pulsed).

There are two different strategies to overcome the limitations of the non-thermal gas-phase plasma:

1. the introduction of ferroelectric pellets into the discharge zone (packed bed) to shift the distribution of accelerated electrons towards higher energies,
2. a synergetic utilisation of plasma processes and heterogeneous catalysis (in-plasma catalysis) by deploying a catalyst in the discharge zone.

The amplification of the electric fields (by a factor of 10–250)[23] and, as a consequence, the formation of higher-energetic species in the discharge

zone is regarded as a main advantage of the usage of ferroelectric pellets. The application of ferroelectric pellets in an NTP has often been described in the literature.[2,5,24–26] In some cases (e.g. the oxidation of benzene[24] and phenol),[27] a higher efficiency in comparison with the conventional gas-phase plasma was achieved, whereas for the oxidation of pcumene and diethyl ether, lower degrees of conversion were observed.[24]

The interpretation of the phenomena occurring with in-plasma catalysis is rather difficult, especially when additionally taking into account the effects of the solid on the discharge characteristics.[28]

In a former paper,[29] we could show (by studying the oxidation of various organic substances immobilised on non-porous and porous catalysts) that short-lived oxidising species formed in the NTP exist in the inner volume of porous materials. This finding can be considered as a pre-requisite for the use of plasma catalysis including its inherent synergetic potential.[27,29] Meanwhile, in-plasma catalysis has been shown to enhance the removal and total oxidation of various compounds such as benzene (with various TiO_2 catalysts[30] or alumina and zeolites),[31,32] toluene (also with TiO_2),[33,34] 2-heptanone (using platinum supported on alumina),[35] chlorinated compounds (using zeolites and vanadium oxide)[8] and perfluorinated compounds (using a commercial mixed-oxide catalyst).[36] In this study, the influence of the application of ferroelectric pellets on various characteristic plasma parameters such as specific energy input and ozone formation as well as the consequences for the conversion of organic compounds were examined.

In particular, the degrees of removal and the selectivity towards CO_2 formation of the packed-bed and the gas-phase reactors for the oxidation of methyl *tert*-butyl ether (MTBE), toluene and a toluene/acetone mixture were investigated.

Finally, various possibilities for the combination of ferroelectric and catalytically active pellets (namely $LaCoO_3$) in NTP were studied with respect to the desired performance for VOC (phenol and MTBE) removal.

2. EXPERIMENTAL

2.1. Materials

All organic test substances (toluene, phenol, MTBE and acetone) were provided by Merck (purity: analytical reagent grade).

Two different ferroelectric materials with perovskite structure were applied without further pretreatment; $BaTiO_3$ and $PbZrO_3$–$PbTiO_3$ (both from Marco GmbH, Hermsdorf, Germany). The $LaCoO_3$ catalyst was tested as received from KataLeuna (Leuna, Germany).

Table I. Physical Parameters of the Inert, Ferroelectric and Catalytically Active Packing Materials

Material	Porosity[a]	Bulk density $g\,cm^{-3}$	Relative dielectric constant	Particle size μm	Specific surface area $m^2\,g^{-1}$
Glass beads	0.39	2.2	5	5000	<0.01
$BaTiO_3$	0.46	5.7	≈3000	1000 . . . 1600	<0.01
$PbZrO_3$–$PbTiO_3$	0.47	7.8	2000	≈ 5000	<0.01
$LaCoO_3$	0.89	5.7	5	500 . . . 3000	20.5[b]

[a]Porosity (including intra- and interparticle pore volumes) determined by gravimetric measurements.
[b]Determined by BET analysis (adsorption/desorption of nitrogen).

The physical parameters of the packed-bed materials are summarised in Table I. The specific surface areas were determined with a Micromeretics ASAP 2000 analyser using the BET method.

2.2. NTP Reactors and Power Supply

For all experiments, coaxial dielectric-barrier-discharge reactors were used.

Reactor R1 consisted of a glass barrier, a tungsten wire (diameter 125μm) as inner electrode and a water jacket as outer electrode.

The reactors R2, R4 and R5 had an inner electrode with a diameter of 5 mm made of stainless steel whereas the inner electrode of the reactor R3 consisted of a stainless-steel cylinder providing a discharge gap of only 1.5 mm. The outer electrode was realised by an aluminium foil for R2 to R5. The physical parameters of the plasma reactors applied are listed in Table II.

Table II. Geometrical and Physical Parameters of the Plasma Reactors

Reactor	Discharge gap mm	Length of the discharge zone mm	Barrier thickness mm	Reactor volume cm^3	Barrier material	Relative dielectric constant of the barrier[a]
R1	5	110	0.5	9	Glass	5
R2	8	430	7	119	Steatite	6
R3	1.5	245	4	70	Glass	5
R4	14	320	7	270	Al_2O_3	9
R5	10	500	4	225	TiO_2	40 . . . 100

[a]Relative dielectric constant measured at a frequency between 48 and 62 Hz.

For all experiments with R1, with the exception of the combination studies (Section 3.4.), high-voltage pulses (duration 11μs, repetition rate 600 Hz) from a pulse generator (Anseros Tübingen, Germany) were used. The other studies (using R2 to R5) were carried out with a high-voltage supply (WGT-301, HCK GmbH Essen, Germany) having a sinusoidal (50 Hz) characteristic.

The power input into the NTP was measured by evaluating the Lissajous figures using a GE 3830 high-voltage probe (Elditest Nürnberg, Germany).

The gas temperature in the packed-bed reactor was measured by means of fibre-optical sensors (OPTOcon Dresden, Germany):[37] it never exceeded 60°C. The barrier and the bulk-phase temperature inside the reactor were found to be nearly identical.

2.3. Gas-flow System and Gas Analysis

Compressed air available in the laboratory was dried and cleaned via columns of $CaCl_2$, supported NaOH (both from Merck) and activated carbon before utilisation as carrier gas. The gas flow was controlled by electronic gas-flow controllers (GFC, Bronckhorst Ruurlo, Netherlands) and adjusted to provide a similar residence time for comparable experiments. The concentrations of volatile contaminants were regulated by establishing appropriate temperatures in saturation units.

CO and CO_2 analyses were performed using IR sensors (Multor 610, Maihak Hamburg, Germany; CO_x values every 20 s). The ozone concentration was monitored by evaluating the UV absorption at 253 nm (Ozomat MP, Anseros Tübingen, Germany).

After the reactors, the gas flow was led to the CO/CO_2 analyser either directly or via a combustion furnace (total-oxidation furnace – TOF; CuO at 700°C; for details see Ref. 29). This arrangement allowed the measurement of the CO_x concentrations as well as the total carbon content in the effluent gas streams. The concentration of emitted VOCs could be deduced from the difference between these two values.

The quantitative analyses of the toluene and acetone concentrations during the selectivity studies were performed using a gas chromatograph (DANI 86.10 HAT-GC) equipped with a thick-film column (Optima-1-DF-l.00; 25 m $\times$ 0.32 mm, Macherey & Nagel). The detector temperature was set to 280°C. In order to avoid the post-plasma decomposition of ozone and the oxidation of acetone and toluene in the injector and the column, injector and column were operated isothermally at 50°C. The injected sample volume was 250μL.

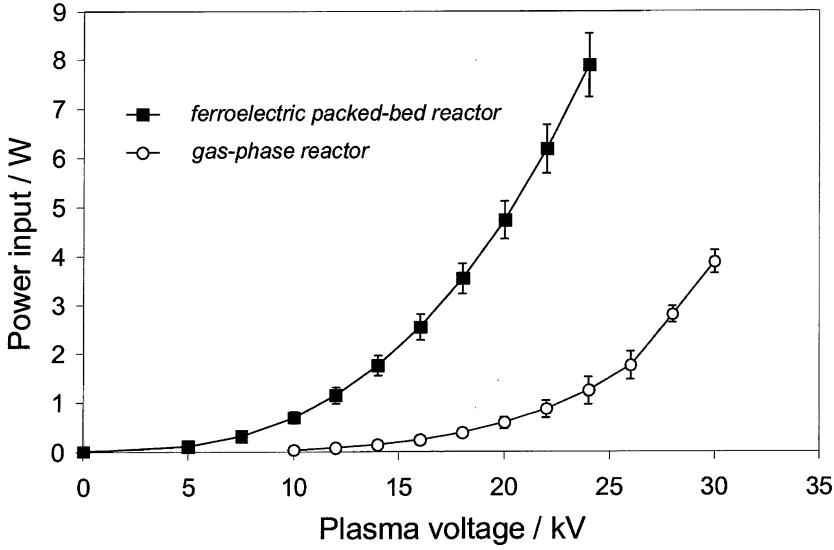

Fig. 1. Energy input as a function of applied high voltage for the gas-phase and the ferroelectric packed-bed reactors (synthetic-air atmosphere, reactor type R1, pulsed high voltage with 600 Hz, residence time 3.5 s, 30 g $BaTiO_3$ as pellets).

3. RESULTS AND DISCUSSION

3.1. Energy Input and Ozone Formation

Figure 1 shows the energy input for the gas-phase and the ferroelectric packed-bed reactors (R1) as a function of the applied high voltage. The specific energy input in a reactor filled with ferroelectric pellets is considerably higher (by a factor of 6–10 at higher voltages) than in a gas-phase reactor. The higher energy input can either be explained by dielectric losses (dielectric heating of the ferroelectric pellets based on a principle similar to heating in a microwave oven) or changes in the characteristics of the discharge processes in the plasma. However, the corresponding model calculations based on frequency-dependent dielectric and hysteresis measurements showed that, in the relevant voltage range, less than 3% of the energy input is expended in for dielectric heating[38] Therefore, the altered behaviour when introducing ferroelectric pellets into the discharge zone of a NTP can be ascribed to more discharges per reactor volume (additional micro-discharges) and/or discharges having a higher energy density.

A remarkable consequence of the introduction of a ferroelectric packed-bed is that the ozone concentration curves are characterised by a

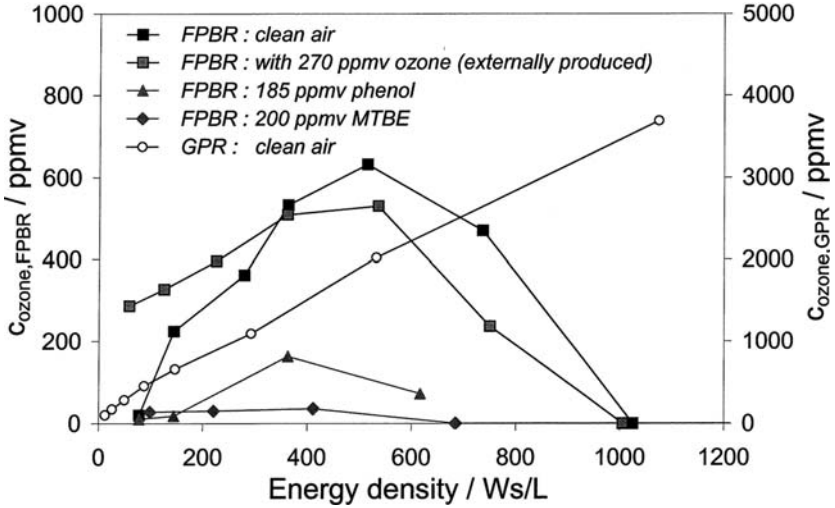

Fig. 2. Ozone concentration in the effluent of a gas-phase reactor (GPR, only clean air) and a ferroelectric packed-bed reactor (FPBR) as a function of energy density during treatment of clean synthetic air and air containing ozone, phenol and MTBE (for experimental details, see explanations in Fig. 1).

maximum at medium energy densities (e.g. at about 500 Ws/L in Fig. 2) and the total absence of ozone emission from the reactor at higher energy densities (above 1000 Ws/L). This behaviour (most likely due to a thermally initiated decomposition) is in good agreement with former studies by Yamamoto *et al.*,[39] also using a $BaTiO_3$ packed bed. In contrast, the gas-phase NTP reactor showed a steadily increasing ozone concentration in the effluent up to the highest applied energy densities (1100 Ws/L).

As also shown in Fig. 2, even externally produced ozone (input concentration 270 ppmv) is effectively destroyed in the ferroelectric packed-bed reactor. Taking into account this potential for O_3 decomposition, it is likely that ozone is still produced at higher specific energy input (above 100 Ws/L). However, its lifetime is considerably reduced and, therefore, it could not be detected at the outlet of the NTP reactor.

In the presence of hydrocarbons (phenol and MTBE), the ozone concentration was much lower and no ozone was detectable at energy densities above about 700 Ws/L. This implies that ozone and ozone precursors, namely triplet oxygen species $O(^3P)$, were consumed during the oxidation of MTBE and phenol.

For comparison, the conventional ozone destruction was studied as a function of temperature by placing the same ferroelectric packed-bed

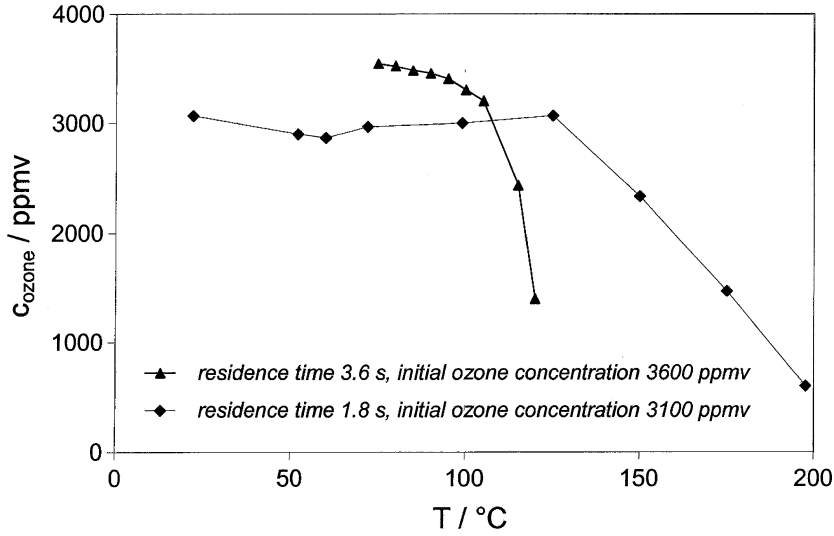

Fig. 3. Ozone decomposition by a $BaTiO_3$ packed bed as a function of temperature established in a conventional furnace for two different residence times.

reactor (R1) in a furnace. The concentration of ozone-containing air at the entrance of the packed bed (3000–3600 ppmv, produced in an additional NTP reactor) was significantly reduced at temperatures above 100°C (Fig. 3), which is in good agreement with studies by Chae *et al.*[24] using an ozone decomposer. They have shown that with increasing temperature the ozone generation was reduced and the ozone loss processes were enhanced. As expected, the degradation of ozone was larger for a longer residence time in the packed-bed reactor.

Because the macroscopic temperature in the bed as measured with a fibre-optical sensor did not exceed 60°C, the ozone decomposition can only be explained by the occurrence of hot spots. These hot spots could be represented by rather small zones which were equally distributed within the ferroelectric bed. These active volumes are presumably formed by strong micro-discharges appearing in particular between sharp edges and corners of adjacent ferroelectric pellets. Due to their small size and the heat transfer by the passing gas stream, the temperature of the ferroelectrie bed obviously did not significantly increase.

3.2. Oxidation of MTBE and Toluene

In order to evaluate the potential of ferroelectric and inert (glass beads) packed-bed materials for enhancing the oxidation of organic

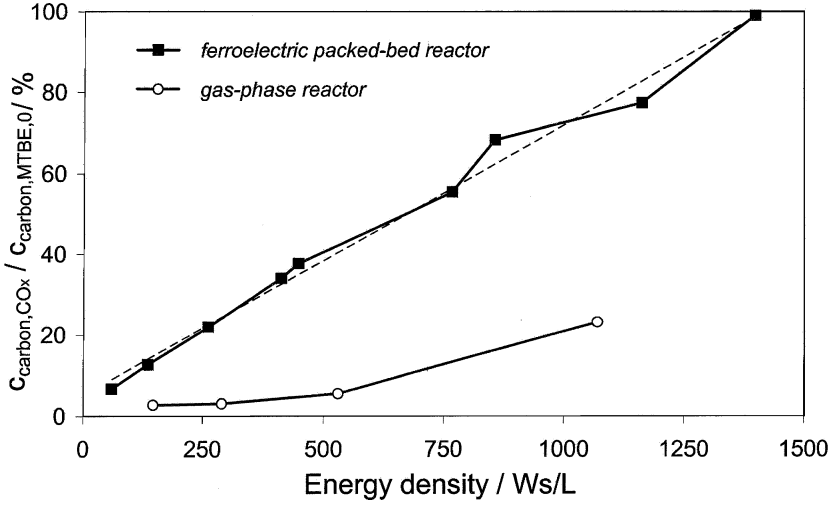

Fig. 4. Conversion of MTBE to carbon oxides (calculated on the basis of the carbon balance) as a function of energy density in a gas-phase and a ferroelectric packed-bed reactor (R1, pulsed high voltage with 600 Hz repetition rate, residence time 3.5 s, 30 g $BaTiO_3$ as pellets, initial MTBE concentration approx. 200 ppmv).

pollutants, the NTP oxidation of MTBE and toluene was studied. As shown in Figs. 4 and 5, the conversion of both hydrocarbons to CO_x was significantly enhanced by the ferroelectric packed-bed material ($BaTiO_3$) in the whole range of specific energy input. The usage of glass beads exhibiting a surface comparable to that of the perovskite did not markedly change the performance of the NTP reactor, confirming the results found in studies by Yamamoto *et al.*[39] The residence time and the flow conditions with both materials were comparable. Therefore, the enhanced surface area or geometric reasons in general can be excluded as the origin of the strong effect observed with a ferroelectric packed bed. Additionally to the increased degree of conversion to CO_x, the formation of polymeric deposits was reduced in the case of toluene.

Figure 6 shows the selectivity to CO_2 formation for the oxidation of MTBE and toluene for both reactor types (for comparison, in Fig. 6 the results for toluene oxidation in a reactor filled with glass beads is also presented). In both cases, a slight increase of the total oxidation (about 10% for toluene and 15–30% for MTBE) was observed. A relatively small increase in the selectivity to total oxidation could also be observed when applying glass beads. However, in spite of the observed improvement, the concentration of CO was still on a par with that of CO_2. Interestingly, an

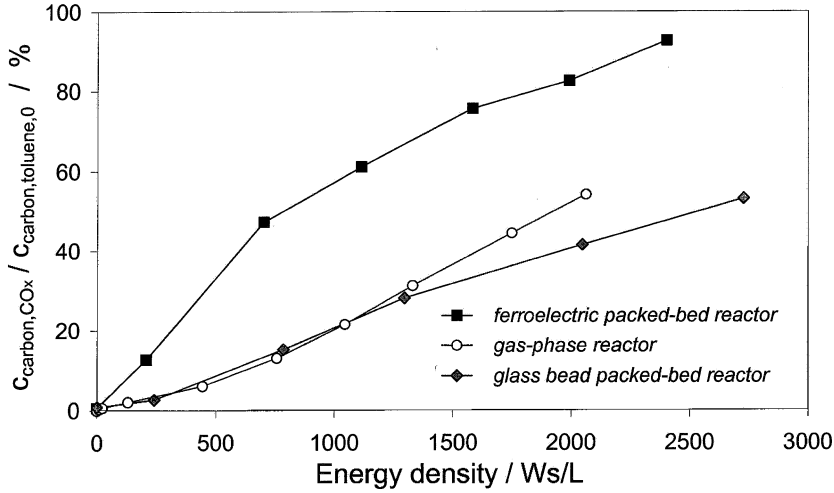

Fig. 5. Conversion of toluene to carbon oxides (calculated on the basis of the carbon balance) as a function of energy density in a gas-phase, a glass-bead packed-bed and a ferroelectric packed-bed reactor (R2, sinusoidal high voltage with 50 Hz, residence time about 30 s, 0.7 kg of $PbZrO_3$–$PbTiO_3$ pellets, initial toluene concentration approx. 450 ppmv).

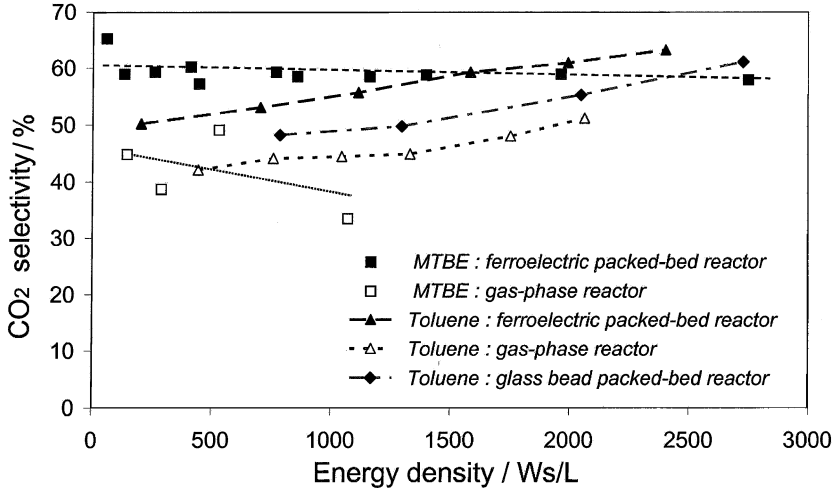

Fig. 6. Selectivity to CO_2 formation for the NTP oxidation of MTBE and toluene as a function of energy density in a gas-phase, a glass-bead packed-bed and a ferroelectric packed-bed reactor (for experimental details, see descriptions in Figs. 4 and 5).

increasing energy input did not noticeably influence the selectivity, implying that the CO_2/CO ratio depends more on the type of hydrocarbon rather than on the energy density.

Therefore, a ferroelectric packed bed is a suitable tool for increasing the energetic efficiency but it is not sufficient for solving the problem of the low extent of total oxidation in the NTP.

3.3. Selectivity Studies

One main goal of these studies was to prove the enhanced formation of higher-energetic reactive species in a ferroelectric packed-bed reactor. In order to clarify this question, a model reaction with two different organic compounds was chosen. The variation of the energy spectrum of the reactive species formed in the NTP should result in a modification of the relative oxidation selectivities. Acetone and toluene were oxidised as a gas mixture in air using several NTP reactors mainly differing in the barrier material and the presence of a ferroelectric bed. Compared to toluene, acetone is the less reactive hydrocarbon. This fact is expressed by the rate constants (at 293 K) for reactions with typical plasma species for acetone (with $O(^3P)$: $k=5 \times 10^5\,L\,mol^{-1}\,s^{-1}$, with OH: $k=0.9 \ldots 1.4 \times 10^8\,L\,mol^{-1}\,s^{-1}$, and with $O(^1D)$: $k=3 \times 10^{11}\,L\,mol^{-1}\,s^{-1}$) and for toluene (with $O(^3P)$: $k=5\times10^7\,L\,mol^{-1}\,s^{-1}$, with OH: $3\times10^9\,L\,mol^{-1}\,s^{-1}$, and with $O(^1D)$: $k=8\times10^{11}\,L\,mol^{-1}\,s^{-1}$).[40]

As a selectivity criterion, the relative rate constant K (selectivity factor), which is the ratio of the experimentally determined first-order rate constants k_{ac} and k_{tol}, was defined. Assuming a pseudo-first-order kinetics for the removal of acetone and toluene, Eq. (2) can be written:

$$K = \frac{k_{tol}}{k_{ac}} = \frac{\ln(1 - X_{tol})}{\ln(1 - X_{ac})}, \tag{2}$$

where the X_i values stand for the degree of removal of both substances in a mixture under identical reaction conditions as determined by GC analysis.

Figure 7 shows the selectivity ratio K as a function of the plasma energy density for three different reactors (R3 [gas-phase reactor with glass barrier], R4 [ferroelectric packed-bed reactor with Al_2O_3 barrier] and R5 [ferroelectric packed-bed reactor with TiO_2 barrier]).

The K values for the gas phase reactor with glass barrier were found to be 1.5–2 times higher than the values of the reactors with ferroelectric packed bed. Different barrier materials with varying dielectric properties (Table II) did not result in significant selectivity changes. Obviously, the introduction of ferroelectric pellets into the discharge zone causes a better

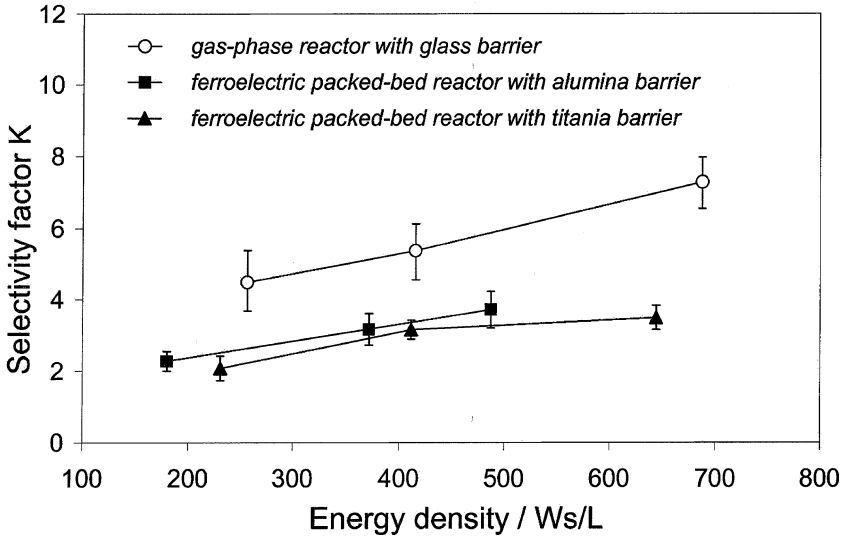

Fig. 7. Selectivity factor K for the oxidation of an acetone/toluene/air mixture as a function of energy density obtained for various reactor setups (R3, R4, R5, sinusoidal high voltage with 50 Hz, toluene and acetone concentrations: 75 ppmv and 160 ppmv, respectively, $PbZrO_3$–$PbTiO_3$ pellets, residence time 10 s).

removal of the less-reactive acetone in comparison to toluene. This shift in the oxidation selectivity cannot be explained by pure quantitative changes of the discharge processes such as an increase in the number of microdischarges per volume. In that case, the removal of both substances would increase similarly.

The most plausible explanation for the selectivity change is a different composition of the pool of reactive species due to a modification of plasma electron energy distribution, in particular a higher mean electron energy in the ferroelectric packed-bed reactors. Presumably, more reactive species are increasingly formed which attack the hydrocarbons less selectively. These conclusions are supported by studies of Liu *et al.* using an electron-energy probe, who found significantly higher mean electron energies close to a zeolite bed in an argon low-pressure plasma.[28]

Obviously, the dielectric constant of the barrier material does not influence the selectivity of the reaction as shown by the comparison of Al_2O_3 ($\varepsilon_r \approx 5$) and TiO_2 ($\varepsilon_r > 40$) in Fig. 7. However, the large value for titania allows lower operating voltages (by a factor of about three for the same power input) which is an advantage for the technical application.

It is remarkable that the selectivity with respect to the hydrocarbons is changed by the ferroelectric packed-bed whereas the ratio between CO and CO_2 also representing the extent of oxidation of carbon monoxide to carbon dioxide is practically unaffected.

3.4. Combination of Ferroelectric and Catalytically Active Packed-bed Materials

In order to combine the advantages of both packing materials, the co-operation of ferroelectric and catalytically active packed-bed materials was studied. Ferroelectric $BaTiO_3$ was applied, mainly enhancing the degree of conversion, whereas $LaCoO_3$ was used as the catalytically active component causing a shift towards total oxidation (i.e. an increase of the selectivity S_{co_2}).[29]

The combination was realised by introducing almost the same volumes of both packed-bed materials either as single-component layers or as a mechanical mixture. The results are exemplarily considered for the conversion of MTBE and two energy densities, namely one mean value of 465 Ws/L (Fig. 8) and the maximum applied value of 930 Ws/L (Fig. 9), which were each used for the different configurations.

The combination of both packing materials in two subsequent layers with $BaTiO_3$ at the entrance and $LaCoO_3$ at the outlet of the NTP reactor (R1) gives the highest conversion to CO_x. However, the extent of CO_x formation was only slightly higher than that occurring with a pure $BaTiO_3$ packing (Figs. 8 and 9). In contrast, the application of an almost homogeneous mixture containing the same volumes of both packed-bed materials (as in the case of the two-layer experiment) resulted in a considerably lower MTBE conversion to CO_x but a higher CO_2 selectivity. Applying only catalytically active $LaCoO_3$, the lowest MTBE conversion and the highest CO_2 selectivity were obtained.

Obviously, a certain co-operation between the two components is established by employing a two-layer reactor. The initial conversion of MTBE to CO_x (and, probably, partially oxidised intermediates) is basically completed in the $BaTiO_3$ layer. The increase of the CO_2 selectivity is preferentially caused by the $LaCoO_3$ pellets, probably due to the further oxidation of such intermediates including CO.

The application of a mechanical mixture as a packed bed (i.e. the distribution of $LaCoO_3$ grains exhibiting a low dielectric constant between the $BaTiO_3$ pellets), seems to reduce the local electric field strengths to such an extent that the whole bed is less effective for oxidising MTBE to CO_x, when compared with the effect of the pure $BaTiO_3$ layer in the two-layer arrangement.

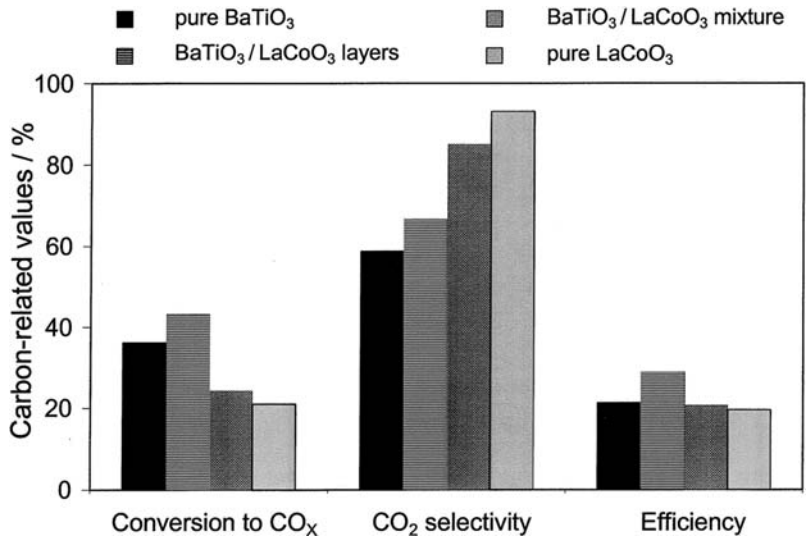

Fig. 8. Degree of conversion to CO_x, selectivity to CO_2 formation and efficiency for total oxidation of MTBE at an energy density of 465 Ws/L with various packed beds in the NTP reactor (R1, sinusoidal high voltage with 50 Hz, 15 g of $BaTiO_3$ and 25 g of $LaCoO_3$, initial MTBE concentration approx. 200 ppmv).

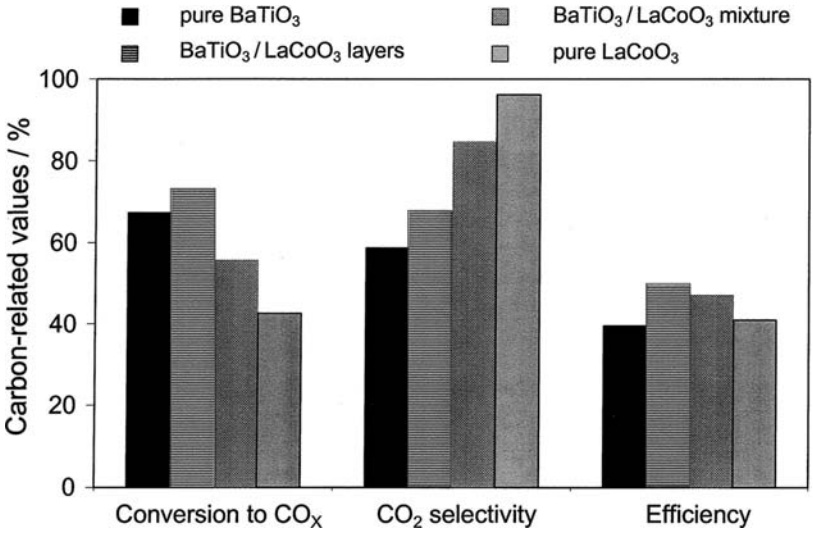

Fig. 9. Degree of conversion to CO_x, selectivity to CO_2 formation and efficiency for total oxidation of MTBE at an energy density of 930 Ws/L with various packed beds in the NTP reactor (same experimental conditions as in Fig. 8).

The oxidation efficiency (defined as the product of conversion to CO_x and CO_2 selectivity, i.e. the CO_2 yield) was the highest in the case of the layered set-up at both energy densities, with a more pronounced result for a medium energy input of 465 Ws/L.

The results emphasise the importance of a beneficial co-operation of ferroelectric and catalytically five packing materials. Obviously, no single one of these solids placed in the discharge zone can alone overcome the limitations of gas-phase plasmas.

Other model experiments carried out with similar two-layer arrangements using phenol showed a much more pronounced effect at maximum energy density, showing that the extent of advantageous synergy effects strongly depends on the contaminants to be eliminated and the energy input.[27]

4. CONCLUSIONS

By comparing the oxidation of various volatile organic compounds in a non-thermal gas-phase plasma reactor and in reactors with ferroelectric and/or catalytically active fillings, the advantageous effect of packed-bed materials in the discharge zone has been demonstrated unambiguously. In particular, the corresponding modifications of a homogeneous gas-phase NTP have a marked influence on the reaction pathways.

In the case of the oxidation of MTBE and toluene, the application of ferroelectric pellets in the discharge zone results in a considerably higher conversion efficiency to CO_x. Studies with glass beads as an almost inert packing material did not show a comparable effect, indicating that the enhanced surface area can be excluded as the origin of the observed influence for a ferroelectric packed bed. Selectivity studies on the oxidation of an acetone/toluene mixture in air provided a strong indication that ferroelectric packing materials considerably enhance the local electric fields in the vicinity of the edges and corners of the packed-bed grains. Consequently, the energy gained by the electrons on their mean free pathway is significantly increased, resulting in a modified energetic pattern of the reactive species.

Although the utilisation of ferroelectric packed beds has been shown to be appropriate for increasing the energetic efficiency, their introduction into the discharge zone is not sufficient for solving the problem of the low degree of total oxidation in the NTP.

Therefore, the application of catalytically active packing materials directly in the discharge zone was studied with the intention of increasing the CO_2 selectivity (plasma catalysis).

Experiments on the combination of the packed-bed materials $BaTiO_3$ (with a high dielectric constant) and catalytically active $LaCoO_3$ (with low dielectric constant) showed that no individual packing material can provide both a high removal degree as well as a high CO_2 selectivity. Combining both solid materials in the NTP in a layered geometry (first layer $BaTiO_3$, second layer $LaCoO_3$) led to the best results concerning the CO_2 yield.

Although conversion to carbon oxides and CO_2 selectivity vary significantly for the various reactor concepts, it is obvious that the overall yield of CO_2 does not. This means that the material effects described in the present paper are not yet at such a level that they can be considered as a solution for technical applications.

Nevertheless, the mechanisms of synergetic interaction occurring in such complex NTP systems bear a great potential for the improvement of NTP applications. However, a great deal of further investigation is required in order to characterise these effects in more detail and to utilise these phenomena for the optimisation of NTP applications.

ACKNOWLEDGMENTS

The authors thank the Deutsche Bundesstiftung Umwelt for the financial support of these studies.

REFERENCES

1. S. Futamura, A. Zhang, G. Prieto, and T. Yamamoto, *IEEE Trans. Ind. Appl.* **34**, 967 (1998).
2. A. Ogata, K. Mizuno, S. Kushiyama, and T. Yamamoto, *Plasma Chem. Plasma Process*. **18**, 383 (1998).
3. A. Ogata, D. Ito, K. Mizuno S. Kushiyama, A. Gal, and T. Yamamoto, *Appl. Catal. A: General* **236**, 9 (2002).
4. V. Demidiouk, S. I. Moon, and J. O. Chae, *Catal. Commun*. **4**, 51 (2003).
5. A. Gervasini and V. Ragaini, *Catal. Today* **60**, 129 (2000).
6. G. Pietro, O. Pietro, K. Mizuno, C. Gay, and T. Yamamoto, *Latin Amer. Appl. Res.* **30**, 27 (1999).
7. Y. F. Wang, W. J. Lee, C. Y. Chen, and L. T. Hsieh, *Environ. Sci. Technol*. **33**, 2234 (1999).
8. T. Oda, *J. Electrostat.* **57**, 293 (2003).
9. A. Gal, M. Kurahashi, and M. Kuzumoto, *J. Phys. D: Appl. Phys*. **32**, 1163 (1999).
10. K. Kiyokawa, H. Matsuoka, A. Itou, K. Hasegawa, and K. Sugiyama, *Surface Coatings Techn*. **112**, 25 (1999).
11. R. Li, Y. Keping, J. Miao, and X. Wu, *Chem. Eng. Sci*. **53**, 1529 (1998).
12. T. Hammer, T. Kappes, and M. Baldauf, *Catal. Today* **89**, 5 (2004).
13. B. Rajanikanth, M. Okumoto, S. Katsura, and A. Mizuno, *Proc. IEEE Ann. Meeting 1995*, p. 1813 (1995).

14. L. M. Zhou, B. Xue, U. Kogelschatz, and B. Eliasson, *Plasma Chem. Plasma Process*. **18**, 375 (1998).
15. W. Cho, Y. Baek, S. K. Moon, and Y. C. Kim, *Catal. Today* **74**, 207 (2002).
16. M. Kraus, B. Eliasson, U. Kogelschatz, and A. Wokaun, *Phys. Chem. Chem. Phys.* **3**, 294 (2001)
17. S.-S. Kim, H. Lee, B.-K. Na, and H. K. Song, *Catal. Today* **89**, 193 (2004).
18. B. M. Penetrante, M. C. Hsiao, B. T. Merritt, G. E. Vogtlin, and P. H. Wallmann, *IEEE Trans. Plasma Sci.* **23**, 679 (1995).
19. A. Gervasini, C. L. Bianchi, and V. Ragani, *ACS Symp. Series* **552**, 353 (1994).
20. S. A. Vitale, K. Hadidi, D. R. Cohn, and L. Bromberg, *J. Appl, Phys*. **81**, 2863 (1997).
21. B. M. Penetrante, M. C. Hsiao, B. T. Merritt, G. E. Vogtlin, and P. H. Wallmann, *IEEE Trans. Plasma Sci.* **23**, 679 (1995).
22. B. M. Penetrante, M. C. Hsiao, B. T. Merritt, G. E. Vogtlin, M. Neiger, O. Wolf, T. Hammer, and S. Boer, *Appl. Phys. Lett.* **68**, 3719 (1996).
23. W. Heat and J. Birmingham, *Report, U.S. Department of Energy* (1995).
24. J. Chae, S. Moon, H. Sun, K. Kim, V. Vassiliev, and B. Mikholap, *KSME Int. J.* **13**, 647 (1999).
25. A. Ogata, K. Yamanouchi, K. Mizuno, S. Kushiyama, and T. Yamamoto, *Plasma Chem. Plasma Process*. **19**, 383 (1999).
26. H. Kobno, A. Berezin, J.-S. Chang, M. Tamura, T. Yamamoto, A. Shibuya, and S. Honda, *IEEE Trans. Ind. Appl.* **34**, 953 (1998).
27. U. Roland, F. Holzer, and F.-D. Kopinke, *Catal. Today* **73**, 315 (2002).
28. C.-J. Liu, J.-X. Wang, K.-I. Yu, B. Eliasson, Q. Xia, B. Xue, and Y.-H. Zhang, *J. Electrostat*. **54**, 149 (2002).
29. F. Holzer, U. Roland, and F.-D. Kopinke, *Appl. Catal. B: Environ*. **38**, 163 (2002).
30. S. Futamura, H. Einaga, H. Kabashima, and L. Y. Hwan, *Catal. Today* **89**, 89 (2004).
31. A. Ogata, H. Einaga, H. Kabashima, S. Futamura, S. Kushiyama, and H.-H. Kim, *Appl. Catal. B: Environ.* **46**, 87 (2003).
32. B. Eliasson, K. Zhang, U. Kogelschatz, E. Killer, and B Xue, *EP 1184078* (2000).
33. M. Kang, B.-J. Kim, S. M. Cho, C.-H. Chung, B.-W. Kim, C. Y. Han, and K. J. Yoon, *J. Molecular Catal. A: Chemical* **180**, 125 (2002).
34. D. Li, D. Yakushiji, S. Kanazawa, T. Ohkubo, and Y. Nomoto, *J. Electrostat*. **55**, 311 (2002).
35. C. Ayrault, J. Barrault, N. Blin-Simiand, F. Jorand, S. Pasquiers, A. Rousseau, and J. M. Tatibouët, *Catal, Today* **89**, 75 (2004).
36. M. B. Chang and H. M. Lee, *Catal. Today* **89**, 109 (2004).
37. U. Roland, C. P. Renschen, D. Lippik, F. Stallmach, and P. Holzer, *Sensor Lett.* **1**, 93 (2003).
38. A. Rückauf, *PhD Thesis*, Martin-Luther-Universität Halle-Wittenberg (2002); http://sundoc.bibliothek.uni-halle.de/diss-online/02/02H124/index.htm
39. T. Yamamoto, K. Ramanathan, A. Lawless, D. Ensor, R. Newsome, N. Plaks, and G. Ramsey, *IEEE Trans. Ind. Appl.* **28**, 528 (1992).
40. G. V. Buxton, C. L. Greenstock, W. P. Helman, and A. B. Ross, *J. Phys. Chem. Rev. Data* **17** (1988).